THE JOURNAL OF BIOLOGICAL CHEMISTRY VOL. 286, NO. 27, pp. 23938–23949, July 8, 2011
Printed in the U.S.A.

Increased Lipogenesis and Stearate Accelerate Vascular Calcification in Calcifying Vascular Cells*

Received for publication, March 4, 2011, and in revised form, May 14, 2011 Published, JBC Papers in Press, May 19, 2011, DOI 10.1074/jbc.M111.237065

Tabitha C. Ting[‡], Shinobu Miyazaki-Anzai[‡], Masashi Masuda[‡], Moshe Levi[‡], Linda L. Demer[§], Yin Tintut[§], and Makoto Miyazaki[‡¶1]

From the [‡]Division of Renal Diseases and Hypertension and the [¶]Division of Endocrinology, Diabetes and Metabolism, Department of Medicine, Denver VA Medical Center and University of Colorado, Denver, Aurora, Colorado 80045 and the [§]Division of Cardiology, Department of Medicine, University of California, Los Angeles, California 90095

Vascular calcification is recognized as an independent predictor of cardiovascular mortality, particularly in subjects with chronic kidney disease. However, the pathways by which dysregulation of lipid and mineral metabolism simultaneously occur in this particular population remain unclear. We have shown that activation of the farnesoid X receptor (FXR) blocks mineralization of bovine calcifying vascular cells (CVCs) and in ApoE knock-out mice with 5/6 nephrectomy. In contrast to FXR, this study showed that liver X receptor (LXR) activation by LXR agonists and adenovirus-mediated LXR overexpression by VP16-LXRα and VP16-LXRβ accelerated mineralization of CVCs. Conversely, LXR inhibition by dominant negative (DN) forms of LXRα and LXRβ reduced calcium content in CVCs. The regulation of mineralization by FXR and LXR agonists was highly correlated with changes in lipid accumulation, fatty acid synthesis, and the expression of sterol regulatory element binding protein-1 (SREBP-1). The rate of lipogenesis in CVCs through the SREBP-1c dependent pathway was reduced by FXR activation, but increased by LXR activation. SREBP-1c overexpression augmented mineralization in CVCs, whereas SREBP-1c DN inhibited alkaline phosphatase activity and mineralization induced by LXR agonists. LXR and SREBP-1c activations increased, whereas FXR activation decreased, saturated and monounsaturated fatty acids derived from lipogenesis. In addition, we found that stearate markedly promoted mineralization of CVCs as compared with other fatty acids. Furthermore, inhibition of either acetyl-CoA carboxylase or acyl-CoA synthetase reduced mineralization of CVCs, whereas inhibition of stearoyl-CoA desaturase induced mineralization. Therefore, a stearate metabolite derived from lipogenesis might be a risk factor for the development of vascular calcification.

Saturated fatty acids have often been implicated in the promotion of cardiovascular diseases. Dietary intake and *de novo* lipogenesis are the two major sources of saturated fatty acids. Stearate is one of the most abundant saturated fatty acids in the Western diet (1). Apart from dietary sources, stearate is also endogenously synthesized from acetyl-CoA molecules. *De novo* lipogenesis is a highly regulated process controlled by a number of nutrients and hormones. Although higher rates of lipogenesis occur in liver and adipose tissues, the *de novo* lipogenic pathway is present in all types of mammalian cells. In this pathway, acetyl-CoA carboxylase (ACC)[2] catalyzes the irreversible conversion of the two-carbon acetyl-CoA to the three-carbon intermediate, malonyl-CoA. Malonyl-CoA then serves as the precursor for the endogenous synthesis of fatty acids via the fatty acid synthase (FAS) multi-enzyme complex. FAS catalyzes seven cycles of sequential condensation, reduction, and dehydration reactions to form the 16-carbon saturated fatty acid, palmitate (16:0). Further elongation generally occurs through the actions of microsomal elongases to form stearate (18:0) (2–4).

Vascular calcification is an active cell-mediated process that drives vascular smooth muscle cells to become osteoblast-like cells, and is a major cause of death in patients with chronic kidney disease (CKD) (5, 6). Vascular calcification participates in the formation of atherosclerotic lesions. Previously, vascular calcification was considered a passive and degenerative process causing precipitation of calcium and phosphate, without biological regulation. Vascular calcification is now recognized as the consequence of an actively regulated trans-differentiation of vascular smooth muscle cells into osteoblast-like cells, similar to embryonic bone formation. In addition to phosphate, inflammatory cytokines, and oxidative stress, several *in vitro* and clinical studies have shown lipids to play a crucial role in the pathogenesis of vascular calcification. Lipid-lowering drugs including statins are in fact effective in reducing vascular calcification in several clinical trials (7–9). In vascular calcification, *n*-3 unsaturated fatty acids play a protective role through a p38-MAPK (mitogen-activated protein kinase)-dependent mechanism, whereas oxidized lipids such as oxysterols and oxidized

* This work was supported, in whole or in part, by National Institutes of Health Grants HL081202 and DK081346, the American Heart Association Grant 10BGIA458005, as well as the Colorado Clinical Nutrition Research Unit (National Institutes of Health Grant 5P30DK048520), and the UCHSC Diabetes and Endocrinology Research Center (National Institutes of Health Grant P30DK57516). T. C. T. was supported by NIGMS-IMSD #R25GM083333.

[1] To whom correspondence should be addressed: Dept. of Medicine, Division of Renal Diseases and Hypertension, University of Colorado Denver, 12700 E. 19th Ave., C281 Aurora, CO 80045. Tel.: 303-724-4828; Fax: 303-724-4868; E-mail: Makoto.Miyazaki@ucdenver.edu.

[2] The abbreviations used are: ACC, acetyl-CoA carboxylase; CVCs, calcifying vascular cells; FXR, farnesoid X receptor; LXR, liver X receptor; SREBP, sterol regulatory-binding protein; ALP, alkaline phosphatase; FAS, fatty acid synthase; SCD, stearoyl-CoA desaturase; CKD, chronic kidney disease; ChREBP, carbohydrate response element-binding protein; MOI, multiplicity of infection.

phospholipids elicit procalcific effects in vascular cells. In addition, we previously reported that lipid and calcium accumulation simultaneously occurs during osteogenic differentiation of vascular cells. However, which lipids and by what mechanism lipids cause vascular calcification were not well understood. Whether saturated fatty acids are risk factors in vascular calcification was also heretofore unknown.

A number of transcription factors exert regulatory control over *de novo* lipogenesis, particularly in the liver. Liver X receptor (LXR) is an oxysterol nuclear receptor that regulates cholesterol, glucose, and fatty acid metabolism. There are two isoforms of LXR in humans, LXRα and LXRβ. LXRα (NR1H3) is mostly expressed in liver, intestine and kidney; whereas LXRβ (NR1H2) is ubiquitously expressed (10). Many recent studies using synthetic agonists and knock-out mice have demonstrated that LXR activation elicits anti-atherogenic effects by increasing reverse cholesterol transport, reducing intestinal cholesterol absorption and decreasing inflammation (11–14). Unfortunately, LXR activation also exhibits undesirable effects that cause hypertriglyceridemia and liver steatosis via induction of hepatic *de novo* lipogenesis (15, 16). LXR activates the transcription of lipogenic genes such as fatty acid synthase (FAS), acetyl CoA carboxylase (ACC), and stearoyl-CoA desaturase-1 (SCD-1) (15). Currently, three independent pathways have been shown to contribute to LXR-mediated induction of lipogenesis: 1) LXR directly activates the expression of lipogenic genes such as FAS, ACC, and SCD-1 through LXR response elements in their promoters (17–19), 2) LXR induces sterol regulatory element binding protein (SREBP)-1c, a master transcription factor, which in turn induces lipogenic gene expression (20, 21), and 3) LXR induces carbohydrate response element binding protein (ChREBP), a glucose-sensitive transcription factor that activates lipogenic gene expression (22). The induction of these pathways by LXR activation synergistically enhances hepatic fatty acid and triglyceride synthesis (22). Another adverse effect of LXR activation by its agonists (T0901317 and GW3965) is the augmentation of vascular calcification induced by the PKA pathway in murine aortic cells (23). Oxysterols also promote mineralization in vascular cells. However, the precise mechanism underlying the pro-calcific effects of LXR agonists and whether the pro-lipogenic effects and pro-calcific effects are linked have not been studied.

Farnesoid X receptor (FXR) is a bile acid nuclear receptor that controls lipid and carbohydrate metabolism (24). Although rodents express two isoforms of FXR (FXRα and FXRβ), humans only express one isoform-FXRα (25). Although it is widely known that FXRα is highly expressed in the liver, kidney, and intestines, it is less known that FXRα is also expressed in the vasculature such as in vascular smooth muscle cells (10, 26). Recently, we reported that FXR plays an important role in regulation of vascular calcification. FXR activation by the synthetic FXR ligand INT-747 and by adenovirus-mediated VP16-FXR overexpression blocked mineralization and lipid accumulation of bovine calcifying vascular cells (CVCs) in response to phosphate. In addition, treatment with INT-747 inhibited vascular calcification in ApoE knock-out (KO) mice with CKD (27). In contrast to LXR, SREBP-1c, and ChREBP, FXR is a major negative regulator of hepatic fatty acid biosynthesis, which is mediated in a SHP-SREBP-1c-dependent manner (28, 29).

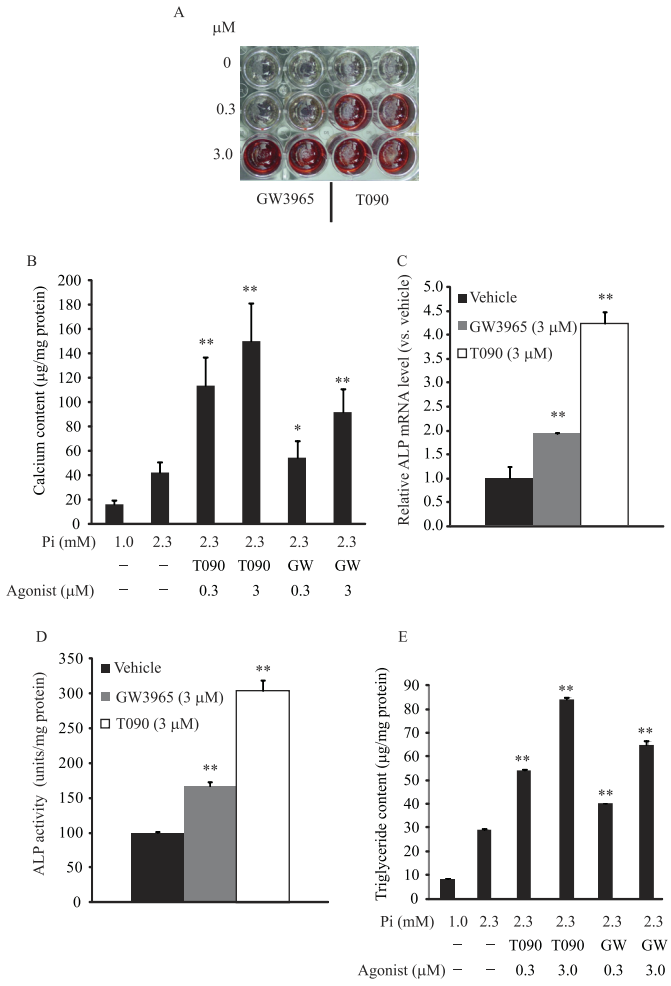

FIGURE 1. **LXR agonists induce mineralization and triglyceride accumulation in CVCs under high phosphate conditions.** CVCs were treated with various concentrations of GW3965 and T0901317 for 14 days in the presence of high phosphate conditions (2.3 mM). *A*, Alizarin Red staining. *B*, calcium content. *C*, ALP mRNA. *D*, ALP activity. *E*, TG content. **, $p < 0.001$ *versus* vehicle with 2.3 mM phosphate. Data represent the mean ± S.E.

In this study, we have addressed three topics: 1) whether FXR decreases and LXR induces lipogenesis through direct and SREBP-1-dependent pathways in vascular cells, 2) whether modification in the lipogenic pathway affects vascular calcification in CVCs, and 3) which fatty acids derived from *de novo* lipogenesis play a major role in the regulation of vascular calcification.

EXPERIMENTAL PROCEDURES

Cell Culture Studies—Bovine calcifying vascular cells (CVCs) were cultured in DMEM containing 15% FBS with either 1.0 mM phosphate (normal phosphate concentration) or 2.0–2.3 mM phosphate (high phosphate concentration). CVCs were treated with 6α-ethyl-chenodeoxycholic acid (INT-747, Intercept Pharmaceuticals Inc., NY), T0901317, 5-(tetradecyloxy)-2-furoic acid (TOFA), CAY10566 (Cayman Chemical), GW3965 (Sigma), triacsin C (Enzo Life Sciences), and free fatty acid-BSA complexes. The fatty acid-BSA complexes were generated as previously described (30). The medium was changed

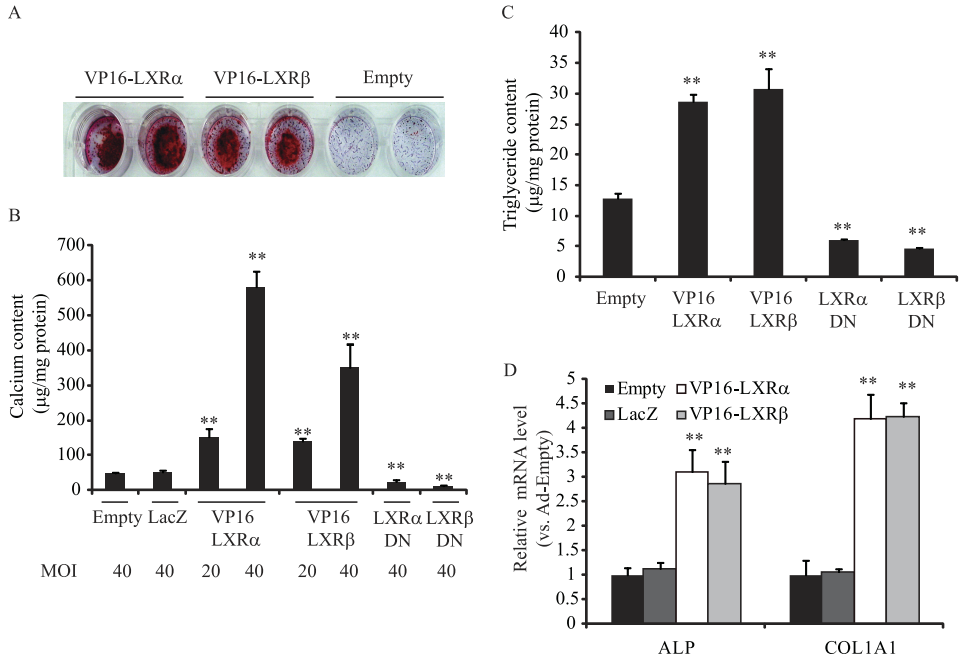

FIGURE 2. **Adenovirus-mediated VP16-LXRα and VP16-LXRβ overexpression accelerate mineralization and triglyceride accumulation, whereas LXRαDN and LXRβDN ameliorate these effects in CVCs under high phosphate.** CVCs were treated with adenoviruses at an MOI of either 20 or 40. After 12 h of adenovirus treatment, the medium was replaced with DMEM containing 15% FBS and 2.0 mM phosphate for 10 days. *A*, Alizarin Red staining. *B*, calcium content. *C*, TG content. *D*, ALP and COL1A1 mRNA. **, $p < 0.001$ *versus* Ad-empty with 2.0 mM phosphate. Data represent the mean ± S.E.

every 2–3 days. Fourteen days after reaching confluence, the cells were stained with Alizarin Red to identify calcium deposits (27).

Calcium Content in Cultured Cells and Aorta—Calcium deposition in the plates was quantified as previously described. Cells were decalcified using a 0.6 M HCl solution. After collecting the supernatant, the cells were washed with PBS and solubilized with a 0.1 N NaOH/0.1% SDS solution for protein quantification. The calcium content was quantified calorimetrically using the *o*-cresolphthalein method. The protein content was measured using a BCA protein assay kit (27).

RNA Analysis—Total RNA was isolated using Tri reagent in conjunction with an RNAeasy kit. Real-time quantitative PCR assays were performed by using an Applied Biosystems StepOne qPCR instrument. In brief, 1 μg of total RNA was reverse transcribed with random hexamers by using the High Quality Reverse Transcription Reagents kit (Applied Biosystems). Each amplification mixture (10 μl) contained 25 ng cDNA, 900 nM forward primer, 900 nM reverse primer, and 5 μl of Universal Fast PCR Master Mix. Primer sequences are available upon request (27).

Adenoviral Transduction for CVCs—Cells were infected with recombinant adenoviruses at a multiplicity of infection (MOI) of 40, unless otherwise indicated. Adenoviruses expressing VP16-FXR, the active form of SREBP-1c (Addgene), SREBP-1c dominant (DN) negative form (31) (Addgene) VP16-LXRα, VP16-LXRβ, LXRα DN, and LXRβ DN were generated using the ViraPower Adenovirus Expression System (Invitrogen). The VP16 domain was incorporated into the N terminus of the proteins. LXRα DN and LXRβ DN were generated as previously described (32). CVCs were infected with adenovirus in DMEM with 15% FBS. After 12–24 h, the infected cells were treated with media containing 2.0 mM phosphate.

Western Blotting—The cell lysates were prepared using RIPA buffer (Cell Signaling). The samples were separated by SDS-PAGE, transferred to a nitrocellulose membrane, and immunoblotted with a SREBP-1 monoclonal antibody (BD Pharmingen), FAS antibody (BD Pharmingen), ABCA1 (Novus), and VP16 monoclonal antibody (Sigma). Samples were visualized using horseradish peroxidase coupled to an anti-mouse secondary antibody, with enhancement by an ECL detection kit.

Lipid Composition—Cholesterol, fatty acids, and triglycerides (TG) from CVCs were analyzed using gas chromatography, as previously described (33).

Lipid Synthesis Rate—To analyze the rates of fatty acid and cholesterol synthesis, CVCs were treated with 500 μM [^{14}C]acetate (0.5 μCi) or 100 μM [^{14}C]stearate-BSA for 6 h. Fatty acids and cholesterol were saponified using sodium hydroxide and separated with thin layer chromatography. The radioactivity fatty acid and cholesterol fractions was measured by a liquid scintillation counter (34).

Alkaline Phosphatase (ALP) Activity—ALP activity was measured using *p*-nitrophenyl phosphate as the substrate (23).

Statistical Analysis—Data were collected from more than three independent experiments and were reported as the means ± S.E. Statistical analysis was performed using the Student's *t* test, and significance was accepted at $p < 0.05$.

RESULTS

LXR Activation Accelerates Phosphate-induced Mineralization and Triglyceride Accumulation in CVCs—To examine whether LXR activation influences phosphate-induced mineralization and osteogenic differentiation of CVCs, CVCs were treated with two synthetic LXR agonists, T0901317 (T090) and GW3965, under high phosphate conditions. Alizarin Red staining showed that treatment of CVCs with either LXR agonist

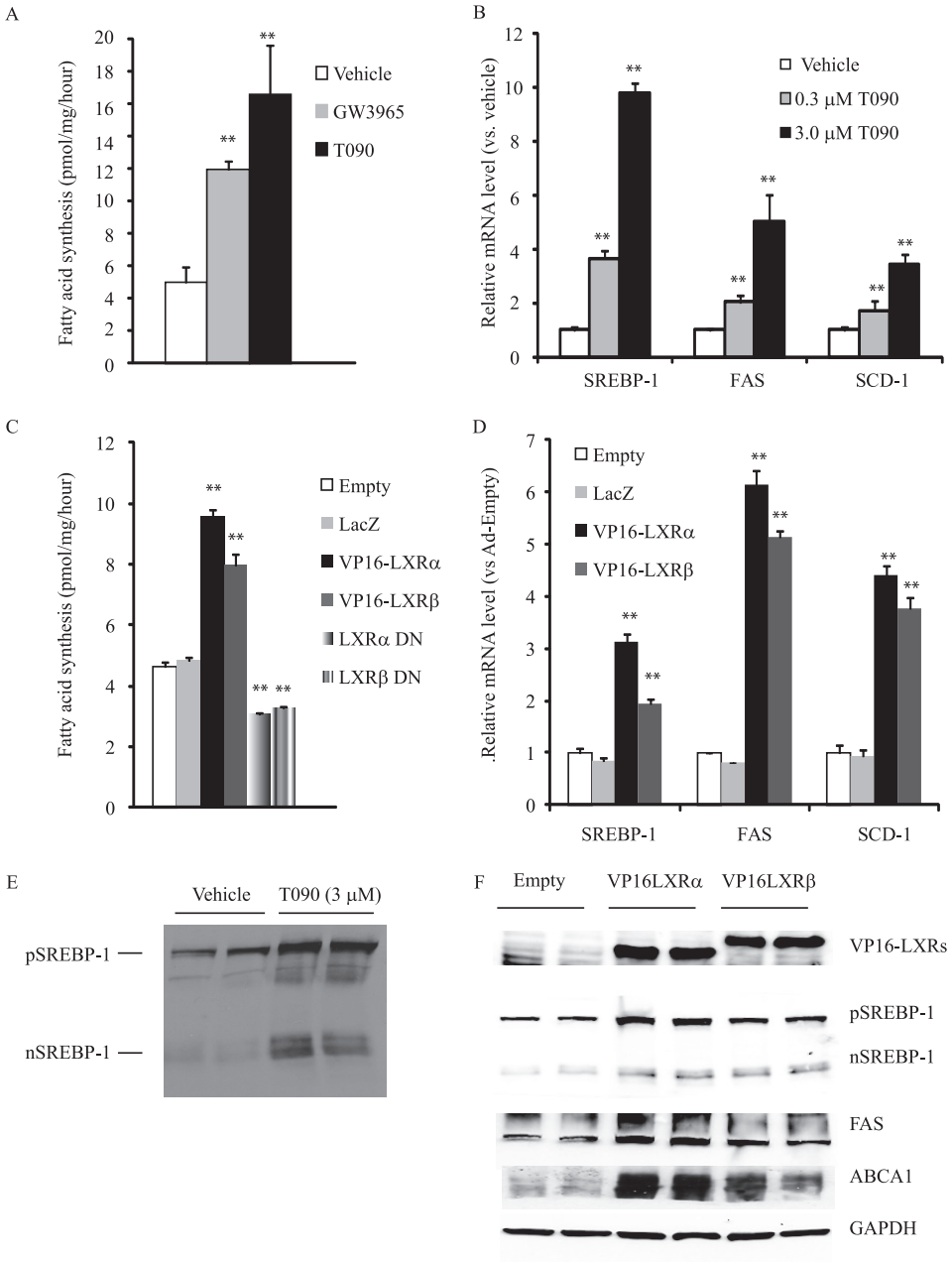

FIGURE 3. **LXR activation by LXR agonists and adenoviruses expressing VP16-LXRs induces *de novo* lipogenesis in CVCs whereas LXRα DN and LXRβ DN reduce it.** *A*, rate of fatty acid synthesis. CVCs were treated with different concentration of GW3965 and T0901317 for 10 days in the presence of high (2.0 mM) phosphate. After 10 days of treatment, CVCs were treated with DMEM containing 0.5 mM [^{14}C]acetate (0.5 μCi) for 6 h. Lipids were extracted, saponified, and separated by TLC. The radioactivity in the fatty acid fractions was analyzed with LSC. **, $p < 0.001$ *versus* vehicle treatment. *B*, SREBP-1 and the target genes in CVCs treated with LXR agonists. *C*, rate of fatty acid synthesis. CVCs were treated with adenoviruses expressing either VP16-LXRs or LXR DNs for 10 days in the presence of high phosphate (2.0 mM). After 10 days of treatment, CVCs were treated with DMEM containing 0.5 mM [^{14}C]acetate (0.5 μCi) for 6 h. Lipids were extracted, saponified, and separated by TLC. Radioactivity in the fatty acid fractions was analyzed with LSC. **, $p < 0.001$ *versus* ad-empty treatment. *D*, SREBP-1 and the target genes in CVCs overexpressing VP16-LXRs and LXR DNs. *E*, SREBP-1 protein in CVCs treated with T090. After 10 days of treatment, total protein was extracted with RIPA buffer containing protease inhibitors and subjected to Western blot analysis with the SREBP-1 monoclonal antibody. pSREBP-1: precursor form of SREBP-1; nSREBP-1: nuclear form of SREBP-1. *F*, VP16-LXRs, SREBP-1, FAS, and ABC1A1 protein expression in CVCs treated with adenovirus expressing VP16-LXRs. Data represent the mean ± S.E.

induced mineralization of CVCs in a dose-dependent manner similar to PKA- induced mineralization (23) (Fig. 1, *A* and *B*). GW3965 and T090 at the 3 μM concentration consistently increased calcium content by 2.1-fold and 3.8-fold, respectively (Fig. 1*B*). GW3965 and T090 treatments also increased ALP mRNA by 1.8-fold and 3.4-fold (Fig. 1*C*), and increased ALP activity by 1.7-fold and 3.0-fold, respectively (Fig. 1*D*). Previously, we reported that triglyceride accumulation occurs simultaneously with mineralization in CVCs treated with high phosphate conditions (27). Therefore, we now examined whether LXR activation increases lipid accumulation in CVCs. We found that CVCs treated with LXR agonists had a significant increase in triglyceride content (Fig. 1*E*), but not in cholesterol content (data not shown). At a 3 μM concentration, GW3965 and T090 treatments increased triglyceride content by 2.2-fold and 2.9-fold, respectively. To determine whether LXRα or

LXRβ activation contributes to mineralization and triglyceride accumulation of CVCs under high phosphate conditions, CVCs were treated with adenoviruses (Ad) expressing either VP16-LXRα or VP16-LXRβ. Remarkably, both VP16-LXRα and VP16-LXRβ overexpression induced mineralization, as assessed by Alizarin red staining (Fig. 2*A*). At a MOI of 40, calcium content increased by 12-fold and 10.7-fold (Fig. 2*B*) and triglyceride content increased by 2.2-fold and 2.3-fold (Fig. 2*C*) in CVCs treated with Ad-VP16-LXRα and Ad-VP16-LXRβ, respectively. VP16-LXRα and VP16-LXRβ significantly induced the expression of ALP and type I collagen (COL1A1) mRNA (Fig. 2*D*). In contrast to LXR activation, inhibition using dominant negative forms (DN) of both LXRα and LXRβ reduced mineralization of CVCs by 51 and 79% and triglyceride accumulation by 54 and 64%, respectively under high phosphate conditions (Fig. 2, *B* and *C*). *LacZ* expression did not affect the mineralization of CVCs (Fig. 2*B*).

LXR Activation Induces de Novo Lipogenesis Whereas FXR Activation Inhibits It—Because LXR activation is known to induce hepatic *de novo* lipogenesis, we reasoned that the activation of lipogenesis in CVCs would increase concentrations of saturated and monounsaturated fatty acids. To examine this hypothesis, we measured the rates of fatty acid and cholesterol synthesis using [^{14}C]acetate. Similar to previous observations of the liver, CVCs treated with GW3965 and T090 compounds exhibited a 2.4-fold and 3.3-fold increase, respectively, in the rate of fatty acid synthesis compared with CVCs treated with the vehicle control (Fig. 3*A*). Ad-VP16-LXRα and VP16-LXRβ treatment increased the rate of fatty acid synthesis by 2.1-fold and 1.7-fold, respectively (Fig. 3*C*) compared with Ad-empty and Ad-LacZ treatment. LXR activation by agonists and VP16-LXRs also increased the rate of cholesterol synthesis (data not shown). The inhibition of LXR by either LXRα DN or LXRβ DN reduced the rate of fatty acid synthesis (Fig. 3*C*). Consistent with the increased rate of *de novo* lipogenesis, mRNAs coding for lipogenic enzymes including FAS and SCD1 were induced by T090 and GW3965 treatment in a dose-dependent manner (Fig. 3*B*). LXR activation also induced mRNA expression encoding SREBP-1 but not ChREBP (Table 1 and 2), which are major transcription factors in the regulation of lipogenic genes (Fig. 3*B* and Table 1). Consistently, the precursor and mature forms of SREBP-1 proteins were increased in CVCs treated with T090 and VP16-LXRα and β (Fig. 3, *E* and *F*). As expected, T090 and GW3965 treatments dramatically induced the expression of ABC transporters ABCA1 and ABCG1 (Table 1). Similar to LXR agonist treatment, Ad-VP16-LXRα and Ad-VP16-LXRβ treatments induced SREBP-1, its target genes (ACC1, FAS, and SCD1) and ABC transporters (ABCA1 and ABCG1) compared with the control treatments such as Ad-empty and Ad-LacZ (Table 2). FAS and ABCA1 protein levels were also higher in CVCs treated with Ad-VP16-LXRα and Ad-VP16-LXRβ (Fig. 3*F*), although the effect of VP16-LXRα was stronger than that of VP16-LXRβ. In contrast to LXR activation, LXR inhibition by the dominant negative forms of LXR reduced mRNA levels for ABC transporters and lipogenic genes (Table 2).

We also analyzed the levels of mRNA encoding proteins involved in vascular calcification. Interestingly, levels of mRNA coding for vitamin K-dependent proteins were reduced by more than 50% in CVCs treated with GW3965 and T090. These vitamin K-dependent proteins including osteocalcin (OCL), matrix γ-carboxyglutamic acid protein (MGP), and osteopontin (OPN) are potent inhibitors of vascular calcification. At a 3 μM concentration, T090 was able to reduced OPN, MGP and OCL mRNA levels by more than 80% (Table 1). VP16-LXRα and VP16-LXRβ also reduced OPN, MGP, and OCL mRNA levels (Table 2). LXR activation induced expression of the sodium-phosphate cotransporter Pit1 and transglutaminases TGM1, TGM2, and TGM5, but not TGM3 (Table 1).

We have previously found that FXR activation inhibits mineralization and osteogenic differentiation of CVCs as well as vascular calcification in ApoE$^{-/-}$ mice with chronic kidney disease (27). Consistent with our previous report, FXR activation by INT-747 (a synthetic agonist of FXR) and VP16-FXR

TABLE 1

Relative amounts of mRNAs in CVCs treated with LXR agonists

CVCs were treated with LXR agonists for 14 days, and the medium was changed every two days. Changes in gene expression are reported as ratios relative to the vehicle control ($n = 6$). Bold type indicates statistical significance ($p < 0.05$ vs. vehicle). Standard errors of the mean were omitted for clarity.

	Vehicle	GW3965	GW3965	T090	T090
		0.3 μM	*3.0 μM*	*0.3 μM*	*3.0 μM*
ABCA1	1.00	**14.85**	**21.41**	**26.66**	**48.21**
ABCG1	ND[a]	**52.45**	**141.73**	**210.34**	**275.05**
ALP	1.00	1.32	**1.94**	**1.81**	**3.43**
Msx2	1.00	0.85	1.28	1.28	**1.46**
Runx2	1.00	0.84	0.85	0.86	0.90
Osx	1.00	1.09	1.07	1.12	1.29
MGP	1.00	**0.19**	**0.21**	**0.18**	**0.07**
OCL	1.00	**0.43**	**0.47**	**0.25**	**0.09**
OPN	1.00	**0.52**	**0.31**	**0.39**	**0.18**
OPG	1.00	0.88	0.82	1.09	**1.85**
Pit1	1.00	1.05	**1.64**	1.34	**2.20**
Pit2	1.00	0.92	1.03	1.01	1.20
Tgm1	1.00	**2.26**	**2.57**	**3.59**	**6.20**
Tgm2	1.00	1.20	1.33	1.41	**12.34**
Tgm3	1.00	0.97	1.02	1.11	1.35
Tgm5	1.00	1.34	**3.19**	**6.43**	**18.18**
SREBP-1	1.00	**2.98**	**3.77**	**3.26**	**7.59**
FAS	1.00	**2.15**	**2.63**	**1.83**	**3.99**
SCD-1	1.00	1.21	**1.51**	**1.53**	**2.64**
ChREBP	1.00	0.98	0.83	1.02	0.94

[a] Not detected—ABCG was not detectable in CVCs treated with the vehicle control.

TABLE 2

Relative amounts of mRNAs in CVCs treated with adenoviruses expressing either VP16-LXRs or LXR DNs

Changes in gene expression are reported as ratios relative to Ad-empty. Bold type indicates statistical significance ($p < 0.05$ vs. vehicle). Standard errors of the mean were omitted for clarity.

	Empty	LacZ	VP16-LXRα	VP16-LXRβ	LXRα DN	LXRβ DN
MOI	40	40	40	40	40	40
ABCA1	1.00	1.44	**7.62**	**8.59**	**0.52**	**0.61**
ABCG1	ND[a]	ND	**453.51**	**52.40**	ND	ND
ALP	1.00	1.20	**2.94**	**2.65**	**0.65**	**0.56**
COL1A1	1.00	0.99	**1.76**	**2.26**	**0.67**	**0.59**
Msx2	1.00	1.19	1.44	**2.46**	1.28	1.08
Runx2	1.00	1.00	0.92	0.93	**0.59**	**0.74**
MGP	1.00	**1.12**	**0.54**	**0.61**	1.16	0.95
OCL	1.00	**1.07**	**0.58**	**0.66**	0.99	1.08
OPN	1.00	1.12	0.6	0.58	1.23	1.33
SREBP-1	1.00	0.82	**1.80**	**2.10**	**0.57**	**0.65**
SREBP-2	1.00	0.99	1.27	1.47	0.95	1.27
ACC1	1.00	1.18	**2.72**	**4.14**	**0.74**	**0.61**
FAS	1.00	1.13	**5.47**	**7.32**	**0.39**	**0.59**
SCD-1	1.00	1.08	**4.60**	**4.03**	**0.54**	**0.55**
ChREBP	1.00	1.59	1.18	1.29	0.97	1.07

[a] Not detected—ABCG was not detectable in CVCs treated with Ad-empty, Ad-LacZ, and Ad-LXR DNs.

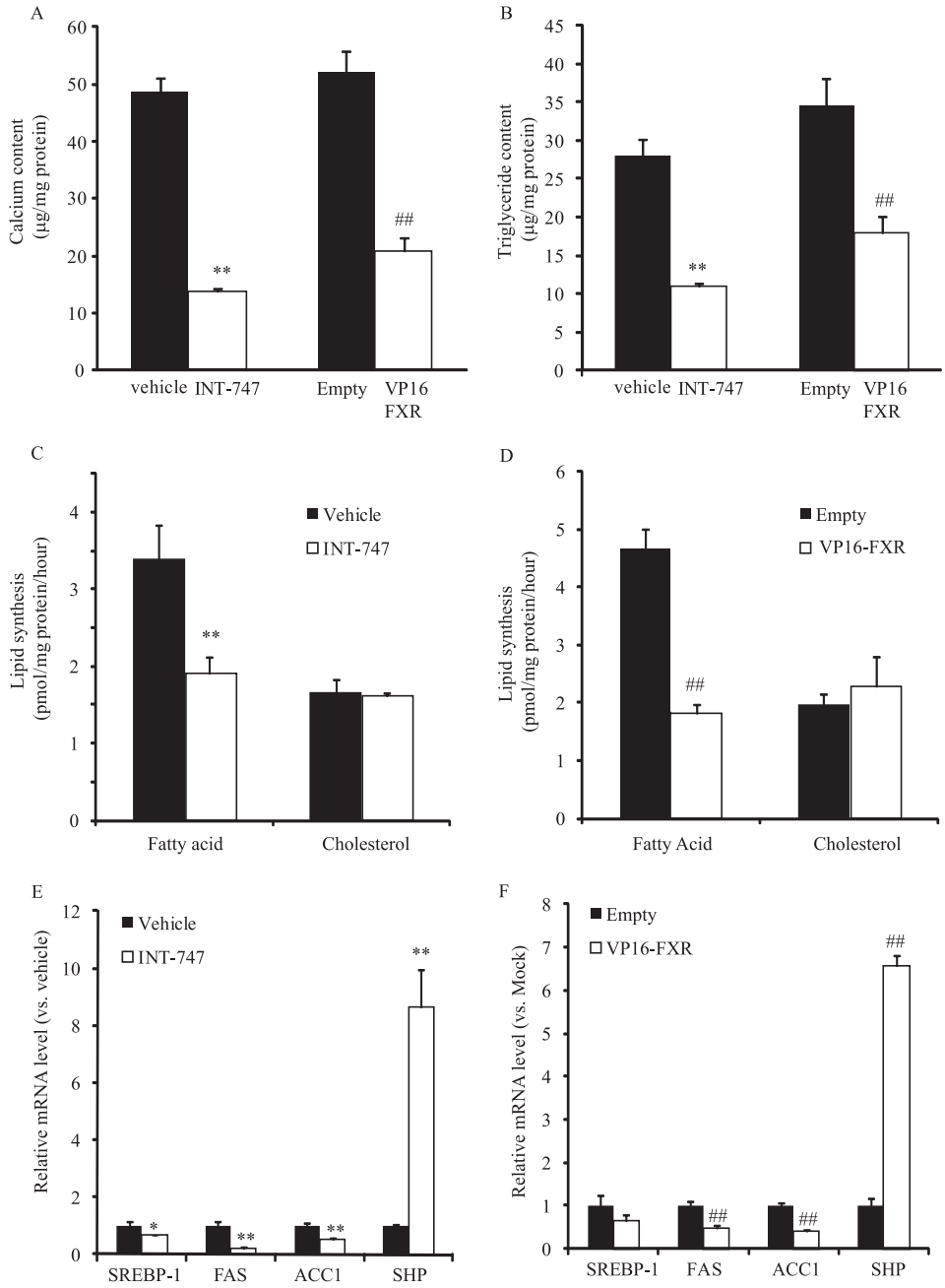

FIGURE 4. **FXR activation by FXR agonist and VP16-FXR reduces mineralization and triglyceride accumulation by reducing SREBP-1 expression and *de novo* lipogenesis.** CVCs were treated with INT-747 (3 μM) and adenovirus expressing VP16-FXR for 14 days in the presence of high (2.0 mM) phosphate. *A*, calcium content. *B*, triglyceride content. *C* and *D*, rates of fatty acid and cholesterol synthesis. After 10 days of treatment, CVCs were treated with DMEM containing 0.5 mM [^{14}C]acetate (0.5 μCi) for 6 h. Lipids were extracted, saponified, and separated by TLC. Radioactivity in the fatty acid fraction was analyzed with LSC. *E*, mRNA levels. Data represent the mean ± S.E. **, $p < 0.001$ *versus* vehicle with 2.0 mM phosphate; ##, $p < 0.001$ *versus* Ad-empty treatment (*Empty*).

decreased calcium content in CVCs by 72 and 63%, respectively (Fig. 4*A*). The triglyceride content of CVCs was also significantly reduced by 61 and 48% in CVCs treated with INT-747 and VP16-FXR, respectively (Fig. 4*B*). INT-747 and VP16-FXR decreased the rate of fatty acid synthesis by 38 and 46%, respectively, but did not decrease cholesterol synthesis (Fig. 4, *C* and *D*). Consistent with the decreased lipogenic rate, the mRNA levels of SREBP-1, FAS, and ACC-1 were significantly decreased by INT-747 (Fig. 4*E*) and by the adenovirus expressing VP16-FXR (Fig. 4*F*).

LXR Activation Increases whereas FXR Activation Decreases Saturated and Monounsaturated Fatty Acids in CVCs—T090 treatment time-dependently increased the levels of saturated and monounsaturated fatty acids palmitate (16:0), palmitoleate [16:1(*n*-7)], stearate (18:0), oleate [18:1(*n*-9)], and vaccenate [18:1(*n*-7)] but not polyunsaturated fatty acids such as linoleate (18:2), linolenate (18:3), arachidonate (20:4), and docosahexaenate (22:6) as compared with vehicle treatment. After 14 days of treatment with T090, there was an increase in 16:0, 16:1(*n*-7), 18:0, 18:1(*n*-9), and 18:1(*n*-7) by 3.0-, 8.7-, 3.5-, 2.7-,

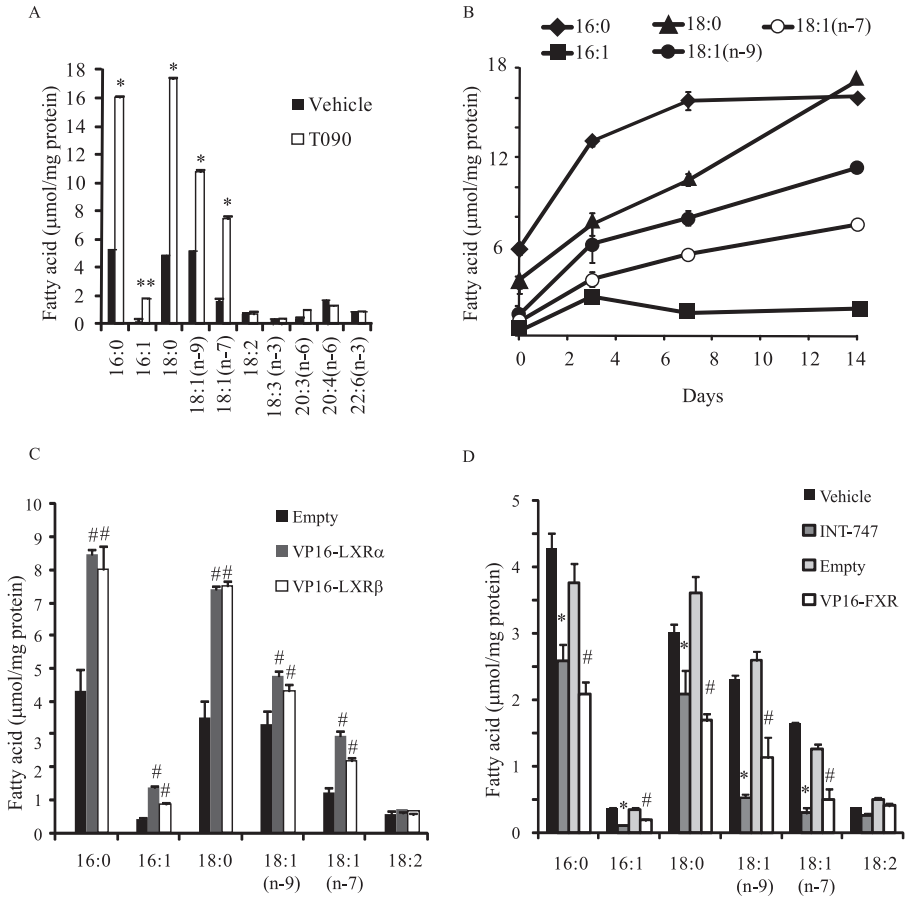

FIGURE 5. **LXR activation increases saturated and monounsaturated fatty acids whereas FXR activation reduces it.** CVCs were treated with T090 (3 μM), INT-747 (3 μM), and adenovirus expressing VP16-LXRs or VP16-FXR for 14 days in the presence of high (2.0 mM) phosphate. Fatty acid levels were analyzed with gas chromatography. *A*, fatty acid levels in CVCs treated with T090 for 14 days. *B*, time course of fatty acid changes by T090 treatment. *C*, fatty acid levels in CVCs treated with an adenovirus expressing either VP16-LXRα or VP16-LXRβ. *D*, fatty acid levels in CVCs treated with either INT-747 at 3 μM or an adenovirus expressing VP16-FXR. CVCs were treated with adenoviruses at a MOI of 40. After 12 h of adenovirus treatment, the media was replaced with DMEM containing 15% FBS and 2.0 mM phosphate for 14 days. *, $p < 0.01$ *versus* vehicle treatment; #, $p < 0.01$ *versus* Ad-empty treatment (*Empty*).

and 4.7-fold, respectively (Fig. 5, *A* and *B*). Similar to T090 treatment, treatment with Ad-VP16-LXRα and Ad-VP16-LXRβ increased those fatty acids derived from *de novo* lipogenesis (Fig. 5*C*). The saturated fatty acids (16:0 and 18:0) were the major fatty acids in differentiated CVCs. In contrast to LXR activation, FXR activation by INT-747 and Ad-VP16-FXR treatment significantly decreased the concentrations of 16:0, 16:1(*n*-7), 18:0, 18:1(*n*-9), and 18:1(*n*-7) (Fig. 5*D*).

SREBP-1 Activation Increases Mineralization and ALP Expression in CVCs—Because SREBP-1 and lipid levels are associated with mineralization of CVCs by LXR activation, we next examined whether the activation of SREBP-1, and the subsequently induced lipogenesis, accelerates mineralization and osteogenic differentiation of CVCs using an adenovirus expressing an active form of SREBP-1c (Ad-nSREBP-1c). CVCs treated with Ad-nSREBP-1c showed a dose-dependent increase in SREBP-1 mRNA and protein (Fig. 6*A*). Active SREBP-1c overexpression increased calcium content in a dose-dependent manner. At a MOI of 40, the treatment of CVCs with Ad-nSREBP-1c for 14 days increased calcium content and ALP mRNA by 2.9-fold and 4.6-fold, respectively compared with the treatment with control adenovirus. In addition, SREBP-1 dominant negative partially reduced mineralization of CVCs induced by T090 treatment.

SREBP-1 Activation Increases the Rate of de Novo Lipogenesis, Lipogenic Gene Expression, the Levels of Triglyceride and Fatty Acids Derived from Lipogenesis—The treatment with Ad-nSREBP-1c increased triglyceride and cholesterol levels by 3.8-fold and 1.8-fold, respectively compared with the empty adenovirus (Fig. 7*A*). The rates of fatty acid and cholesterol synthesis were also significantly increased by 4.5-fold and 3.5-fold, respectively, in CVCs treated with Ad-nSREBP-1c (Fig. 7*B*). Consistent with increased *de novo* lipogenesis, SREBP-1, SCD1, FAS, and ACC1 were induced by 4.2-fold, 7.0-fold, and 5.9-fold, respectively (Fig. 7*C*). In addition, the concentrations of saturated and monounsaturated fatty acids such as 16:0, 16:1(*n*-7), 18:0, 18:1(*n*-9), and 18:1(*n*-7) were increased by nSREBP-1c overexpression (Fig. 7*D*).

Stearate Induces Mineralization of CVCs—Because increased *de novo* lipogenesis is positively correlated with increased mineralization by LXR and SREBP-1 activation, we next examined which fatty acid from *de novo* lipogenesis most induced mineralization of CVCs. We treated CVCs with major fatty acids derived from *de novo* lipogenesis including palmitate (16:0), palmioleate [16:1(*n*-7)], stearate (18:0), oleate [18:1(*n*-9)], and vaccenate [18:1(*n*-7)] at 100 μM, respectively. As a group, these fatty acids showed distinct effects on the mineralization of CVCs. As shown in Fig. 8*A*, saturated fatty acids

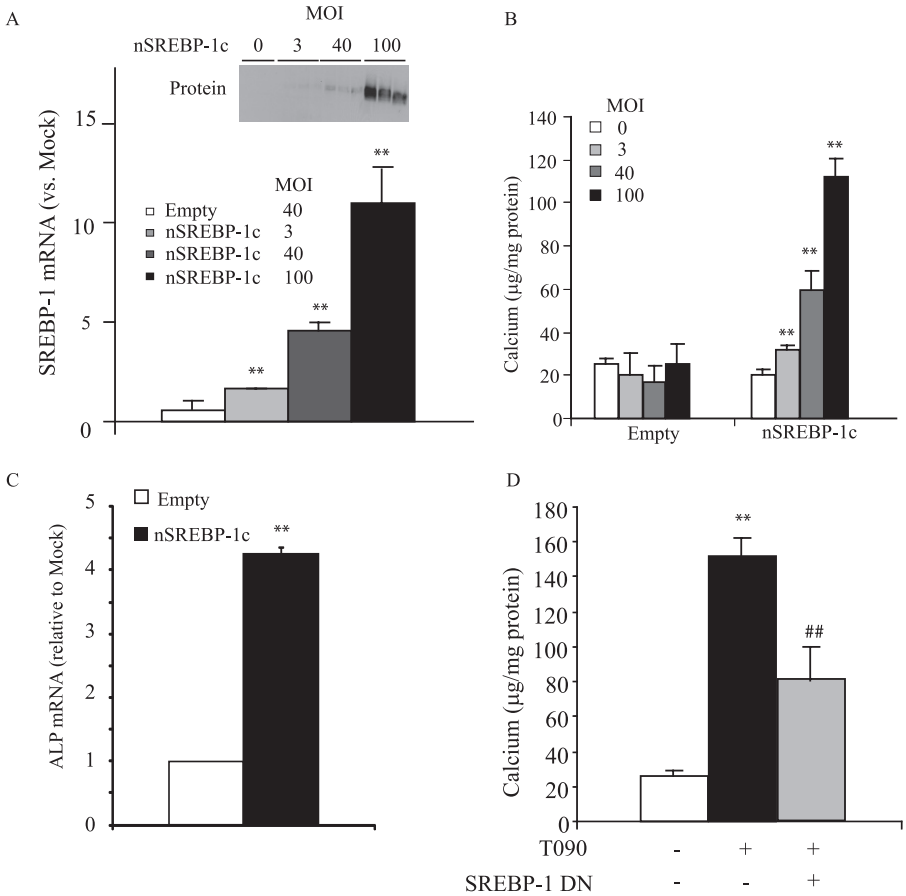

FIGURE 6. **Active SREBP-1c overexpression augments mineralization of CVCs.** CVCs were treated with adenovirus expressing an active form of SREBP-1c (nSREBP-1c) at the indicated MOIs for 14 days. *A*, SREBP-1 mRNA and protein expression in CVCs treated Ad-nSREBP1c. *B*, calcium content in CVCs of adenovirus expressing nSREBP-1. *C*, ALP mRNA. *D*, inhibition of SREBP-1c ameliorates LXR-activation-induced mineralization. CVCs were treated with an adenovirus expressing a dominant negative form of SREBP-1c (SREBP-1c DN) at 40 MOI. After 12 h of adenovirus treatment, the media was replaced with DMEM containing 15% FBS and 2.0 mM phosphate ± 3 μM T090 for 14 days. **, $p < 0.01$ *versus* Ad-empty treatment (Empty); #, $p < 0.01$ *versus* CVCs treated with Ad-empty and 3 μM T090.

palmitate (16:0) and stearate (18:0) significantly increased calcium content. In particular, stearate was very potent at inducing mineralization and increased calcium content in a dose-dependent manner (Fig. 8*B*). At a 200 μM concentration, stearate increased calcium content by 9.1-fold compared with control. Oleate [18:1(*n*-9)] had no effect on mineralization, whereas palmioleate [16:1(*n*-7)] and vaccenate [18:1(*n*-7)] significantly reduced calcium levels in CVCs. In addition, stearate (18:0) induced ALP mRNA and activity when compared with control and oleate [18:1(*n*-9)] (Fig. 8*C*).

Modification of Stearate Metabolism Directly Affects Mineralization of CVC—We next examined whether modification of stearate metabolism directly influences the mineralization of CVCs. Treatment with TOFA (an ACC inhibitor) at 3 μM decreased calcium content by 52% (Fig. 9*A*) in the presence of T090 treatment. The inhibition of stearoyl-CoA desaturase (SCD1) by CAY10566 (1 μM) accelerated mineralization of CVCs induced by either T090 or stearate treatment, whereas the treatment of CVCs with an adenovirus expressing SCD1 completely blocked mineralization (Fig. 9, *A* and *B*). CAY10566 treatment at 1 μM inhibited SCD activity by 97% (data not shown). In addition, the inhibition of acyl-CoA synthetase by triacsin C (5 μM) completely blocked mineralization induced by either T090 or stearate treatment (Fig. 9, *A* and *B*). Triacsin C treatment at 5 μM inhibited triglyceride and cholesteryl ester synthesis by 87 and 62%, respectively (data not shown).

DISCUSSION

Vascular calcification is a major cause of death in patients with CKD (5, 35). The incidence of CKD has dramatically increased in the past decades due to obesity and the diabetes epidemic. Although a number of causative and inhibitory factors for vascular calcification have been identified, the precise mechanism as well as an effective therapy for vascular calcification have not been established. We previously reported that FXR activation by the agonist INT-747 is highly effective in preventing the development of vascular calcification in ApoE$^{-/-}$ mice with CKD (5/6 nephrectomy) and in CVCs (a cell culture model). During osteogenic differentiation, CVCs accumulate not only minerals but also lipids such as triglycerides. The inhibitory effect of FXR agonists is highly correlated with decreased triglyceride content in vasculature (27). The present study was therefore designed to examine the following questions. 1) Where are accumulated lipids in CVCs derived from? 2) Does increased lipogenesis accelerate vascular calcification, and 3) which lipid(s) derived from *de novo* lipogenesis induces vascular calcification? To examine these questions, CVCs were treated with LXR agonists (T090 and GW3965) and

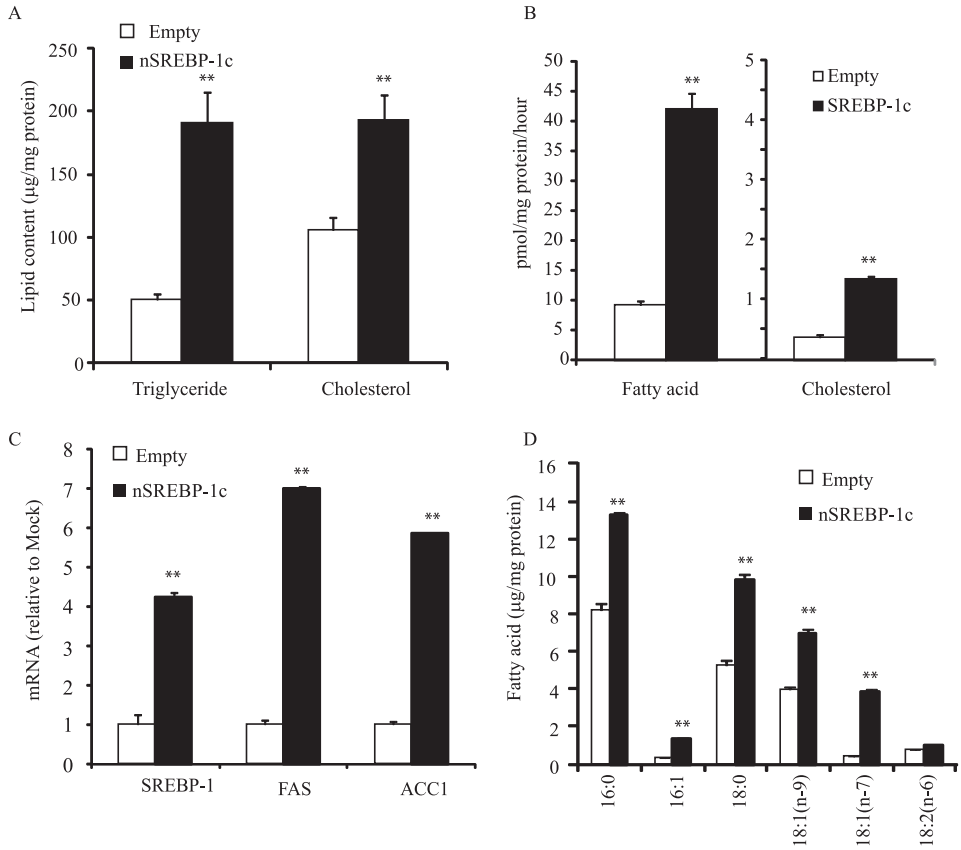

FIGURE 7. **Active SREBP-1c increases triglyceride and fatty acid levels through the induction of lipogenesis.** CVCs were treated with adenovirus expressing an active form of SREBP-1c (nSREBP-1c) at 40 MOI for 14 days. *A*, triglyceride and cholesterol levels in CVCs of adenovirus expressing nSREBP-1c. *B*, rates of fatty acid (*FA*) and cholesterol (*CHOL*) synthesis. *C*, SREBP-1 and target gene mRNA. *D*, fatty acid levels. **, $p < 0.001$ *versus* CVCs treated with Ad-empty.

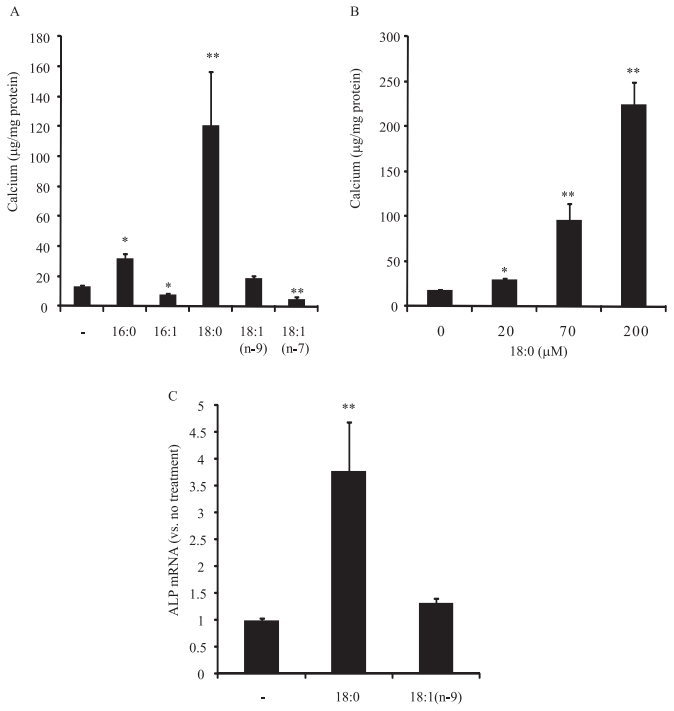

FIGURE 8. **Stearate induces mineralization of CVCs.** CVCs were treated with a fatty acid-BSA complex for 14 days in the presence of high phosphate (2.0 mM). *A*, calcium content in CVCs treated with the indicated fatty acids at 100 μM. *B*, dose-dependent effects of stearate (18:0) on the mineralization of CVCs. *C*, ALP expression induced by stearate (100 μM).

an FXR agonist (INT-747) in the presence of high phosphate conditions. We found that T090 and GW3965 treatment induced mineralization of CVCs in response to high phosphate conditions. ALP mRNA, ALP activity, and triglyceride concentration were simultaneously increased by LXR agonist treatment. In addition, we found that treatment with adenoviruses expressing VP16-LXRs accelerated mineralization and lipid accumulation of CVCs similar to LXR agonist treatment. Since LXR activation induces hepatic lipogenesis, we hypothesized that increased fatty acid synthesis contributes to increased triglycerides content in CVCs treated with LXR agonists. In fact, LXR agonist treatments dramatically increased the rate of fatty acid synthesis and lipogenic gene expression, whereas the rate of fatty acid synthesis and lipogenic gene expression were lowered by INT-747 and VP16-FXR in conjugation with the reduction of mineralization and triglyceride accumulation. There were no significant differences in fatty acid oxidation and uptake (data not shown), suggesting that *de novo* lipogenesis is a major pathway for modulating triglyceride content in CVCs under LXR and FXR activations.

LXR-induced hepatic lipogenesis is mediated through three independent pathways: 1) a direct pathway in which LXR directly induces the expression of lipogenic genes such as FAS, SCD1, and ACC1, 2) an SREBP-1c-dependent pathway and 3) a ChREBP-dependent pathway (18, 21, 22). In CVCs, LXR activation increased protein and mRNA levels of SREBP-1c but not ChREBP. On the other hand, FXR activation is known to reduce

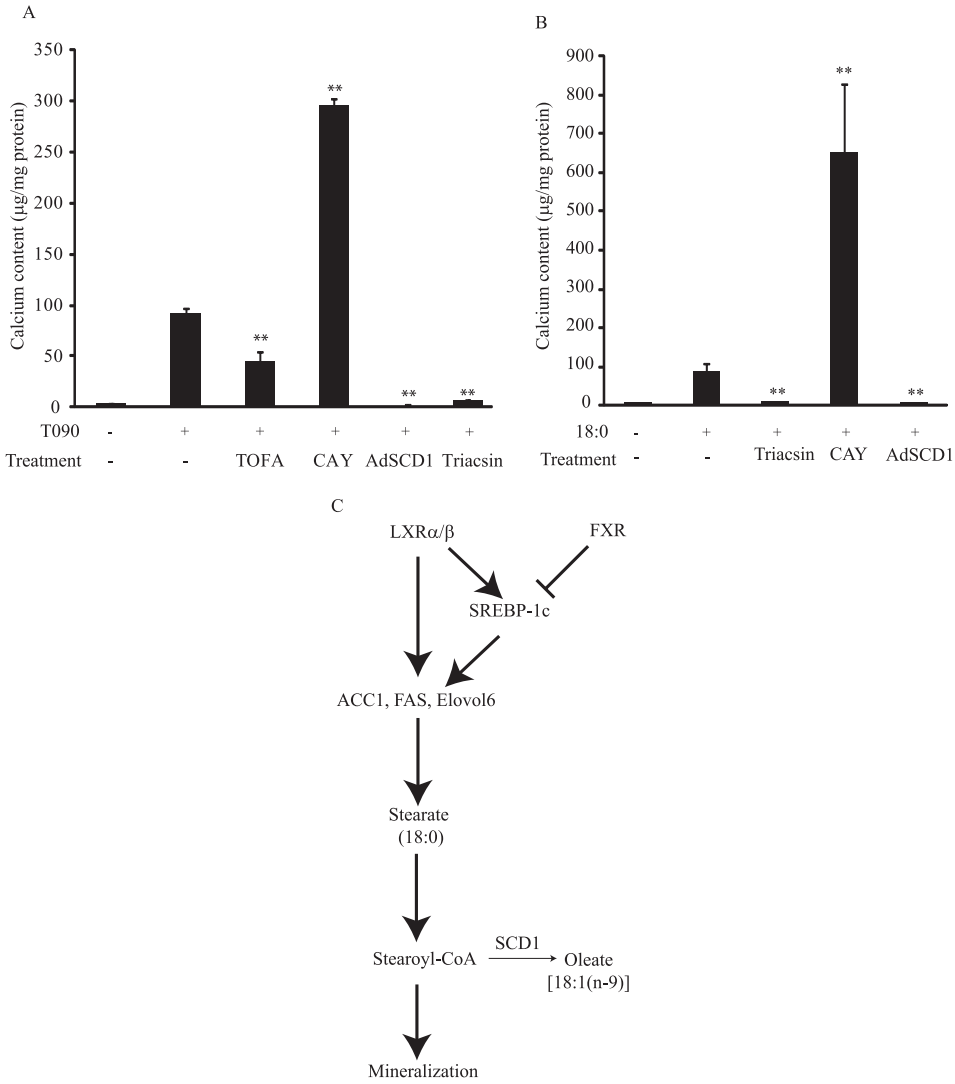

FIGURE 9. **Stearate metabolism in vascular calcification.** *A*, calcium content in CVCs treated with TOFA (3 μM, ACC inhibitor, CAY10566 (1 μM, SCD1 inhibitor), adenovirus expressing SCD1 (Ad-SCD1, MOI 40), and triacsin C (5 μM, acyl-CoA synthetase inhibitor) for 10 days in the presence of T090 (5 μM) and high phosphate (2.3 mM). *B*, calcium content in CVCs treated with CAY10566 (1 μM, SCD1 inhibitor), Adenovirus expressing SCD1 (Ad-SCD1, MOI 40) and triacsin C (5 μM, acyl-CoA synthetase inhibitor) for 5 days in the presence of T090 (5 μM) and high phosphate (2.3 mM). *C*, proposed mechanism for the pro-calcific effect of LXR activation and the anti-calcific effect of FXR activation.

hepatic lipogenesis by inhibiting SREBP-1c. The FXR agonist and VP16-FXR treatment reduced expression of SREBP-1c and its target genes (FAS, ACC, and SCD1) in CVCs just as in the liver. These results suggest that alteration of lipogenesis in CVCs is through direct LXR- and SREBP-1c-dependent pathways. Since both LXRα and LXRβ are expressed in CVCs at similar levels (data not shown), we have also examined whether the LXR isoforms exhibit distinct effects on the mineralization, lipogenesis, and triglyceride accumulation in CVCs. However, LXRα and LXRβ were found to have almost identical effects on mineralization and lipid accumulation in CVCs. Both adenovirus-mediated VP16-LXRα and VP16-LXRβ overexpression accelerated mineralization and lipid accumulation to a similar extent. In addition, LXRα DN and LXRβ DN equally reduced mineralization, lipogenesis, and triglyceride accumulation of CVCs.

Because alteration of SREBP-1c expression and lipogenesis were highly associated with the mineralization of CVCs, we hypothesized that SREBP1c-mediated induction of lipogenesis accelerated mineralization of CVCs. Consistent with our hypothesis, adenovirus-mediated SREBP-1c activation enhanced mineralization and lipid accumulation in CVCs under high phosphate conditions. As expected, SREBP-1c overexpression induced lipogenesis in CVCs. Conversely, either SREBP-1c inhibition by SREBP-1c DN or inhibition of fatty acid synthesis by TOFA partially reduced mineralization of CVCs in response to LXR activation and high phosphate conditions, suggesting that inhibition of SREBP-1c-mediated lipogenesis at least in part obviates the pro-calcific effect of LXR agonists. Thus, we conclude that the lipogenic pathway modulates mineralization and lipid accumulation of CVCs in response to LXR activation.

Consistent with the alteration of lipogenesis and triglyceride content in CVCs, LXR, FXR, and SREBP-1 activation changed the content of saturated fatty acids (16:0 and 18:0) and monounsaturated fatty acids [16:1(*n*-7), 18:1(*n*-9), and 18:1(*n*-7)] in

CVCs. Among the fatty acids that increased in response to *de novo* lipogenesis, saturated fatty acids, particularly stearate (18:0) but not monounsaturated fatty acids strongly and dose-dependently induced mineralization and ALP expression (Fig. 8). Although palmitate also increased calcium content in CVCs to a lesser extent, it might be due to increased stearate levels through the elongation of palmitate. In addition, triacsin C treatment completely blocked mineralization of CVC. The data suggest that changes in stearate-CoA or its metabolite levels control mineralization and osteogenic differentiation in vascular cells, through a mechanism yet to be determined. In a number of previous studies using cell culture systems, saturated fatty acids have been shown to have lipotoxic effects via several cell signaling pathways including 1) endoplasmic reticulum stress (36, 37), 2) Toll-like receptor activation (38–41), 3) an increase in reactive oxygen species (42, 43), 4) *de novo* ceramide synthesis (44–46), 5) modification of mitochondrial structure and function (44, 47), and 6) suppression of anti-apoptotic components (46, 48). In addition, unsaturated fatty acid supplementation has been known to block the lipotoxic effects of saturated fatty acids. We found that *n*-7 monounsaturated fatty acids (MUFAs) such as palmitoleate [16:1(*n*-7)] and vaccenate [18:1(*n*-7)], but not oleate [18:1(*n*-9)], reduced mineralization of CVCs in contrast to stearate. Palmitoleate has been proposed to rescue endoplasmic reticulum stress (37). In addition, the inhibition of MUFA synthesis by an SCD-specific inhibitor (CAY10566) promoted vascular calcification induced by stearate treatment or either LXR agonist, whereas adenovirus-mediated overexpression of SCD1 attenuated vascular calcification. It would be interesting to elucidate which pathway is involved in the pro-calcific effect of stearate and anti-calcific effect of *n*-7 MUFAs, and which of their metabolites mediate their effects.

There is another potential mechanism by which LXR activation might accelerate mineralization of CVCs. LXR activation alters the expression of genes responsible for vascular calcification. Treatment with LXR agonists increases positive regulators of mineralization such as ALP, transglutaminases, and Pit-1, whereas, it very strongly down-regulates the negative regulators such as matrix γ-carboxyglutamic acid protein (MGP), osteocalcin (OCL), and osteopontin (OPN). Similar changes in expression of these genes by LXR agonists have also been reported previously (23). Although it is not known whether LXR directly alters expression of those regulators, increased expression of positive regulators and decreased expression of negative regulators may also contribute to the pro-calcific effect of LXR agonists.

In conclusion, our findings indicate that increased stearate via the induction of *de novo* lipogenesis promotes mineralization of CVCs under pro-osteogenic conditions such as high phosphate levels and LXR activation. As indicated in Fig. 9*C*, we propose that the direct LXR and SREBP-1c-dependent pathways induce lipogenic gene expression in CVCs. The induced lipogenic pathway leads to an increase in stearate level in CVCs. The stearate-CoA or its metabolite(s) mediates the pro-calcific effect of LXR. LXR activation can also induce SCD1 to convert stearate to oleate. This is a protective pathway for stearate-induced mineralization. On the other hand, FXR activation reduces lipogenic gene expression by inhibiting SREBP-1c though SHP (small heterodimer partner) induction. The depressed lipogenic pathway reduces stearate levels which results in the inhibition of CVC mineralization (Fig. 9*C*, *right*). Because LXR activation attenuates atherosclerosis, it would ameliorate atherosclerotic intimal calcification. However, LXR activation could exert adverse effects on medial calcification frequently found in patients with chronic kidney disease.

REFERENCES

1. Sampath, H., and Ntambi, J. M. (2005) *Lipids* **40,** 1187–1191
2. Miyazaki, M., and Ntambi, J. M. (2003) *Prostaglandins Leukot. Essent. Fatty Acids* **68,** 113–121
3. Matsuzaka, T., Shimano, H., Yahagi, N., Yoshikawa, T., Amemiya-Kudo, M., Hasty, A. H., Okazaki, H., Tamura, Y., Iizuka, Y., Ohashi, K., Osuga, J., Takahashi, A., Yato, S., Sone, H., Ishibashi, S., and Yamada, N. (2002) *J. Lipid Res.* **43,** 911–920
4. Moon, Y. A., Shah, N. A., Mohapatra, S., Warrington, J. A., and Horton, J. D. (2001) *J. Biol. Chem.* **276,** 45358–45366
5. Mizobuchi, M., Towler, D., and Slatopolsky, E. (2009) *J. Am. Soc. Nephrol.* **20,** 1453–1464
6. Jono, S., Shioi, A., Ikari, Y., and Nishizawa, Y. (2006) *J. Bone Miner Metab.* **24,** 176–181
7. Callister, T. Q., Raggi, P., Cooil, B., Lippolis, N. J., and Russo, D. J. (1998) *N. Engl. J. Med.* **339,** 1972–1978
8. Sharp Collaborative Group (2010) *Am. Heart J.* **160,** 785–794
9. Achenbach, S., Ropers, D., Pohle, K., Leber, A., Thilo, C., Knez, A., Menendez, T., Maeffert, R., Kusus, M., Regenfus, M., Bickel, A., Haberl, R., Steinbeck, G., Moshage, W., and Daniel, W. G. (2002) *Circulation* **106,** 1077–1082
10. Bookout, A. L., Jeong, Y., Downes, M., Yu, R. T., Evans, R. M., and Mangelsdorf, D. J. (2006) *Cell* **126,** 789–799
11. Tontonoz, P., and Mangelsdorf, D. J. (2003) *Mol. Endocrinol.* **17,** 985–993
12. Joseph, S. B., and Tontonoz, P. (2003) *Curr. Opin. Pharmacol.* **3,** 192–197
13. Joseph, S. B., McKilligin, E., Pei, L., Watson, M. A., Collins, A. R., Laffitte, B. A., Chen, M., Noh, G., Goodman, J., Hagger, G. N., Tran, J., Tippin, T. K., Wang, X., Lusis, A. J., Hsueh, W. A., Law, R. E., Collins, J. L., Willson, T. M., and Tontonoz, P. (2002) *Proc. Natl. Acad. Sci. U.S.A.* **99,** 7604–7609
14. Kratzer, A., Buchebner, M., Pfeifer, T., Becker, T. M., Uray, G., Miyazaki, M., Miyazaki-Anzai, S., Ebner, B., Chandak, P. G., Kadam, R. S., Calayir, E., Rathke, N., Ahammer, H., Radovic, B., Trauner, M., Hoefler, G., Kompella, U. B., Fauler, G., Levi, M., Levak-Frank, S., Kostner, G. M., and Kratky, D. (2009) *J. Lipid Res.* **50,** 312–326
15. Schultz, J. R., Tu, H., Luk, A., Repa, J. J., Medina, J. C., Li, L., Schwendner, S., Wang, S., Thoolen, M., Mangelsdorf, D. J., Lustig, K. D., and Shan, B. (2000) *Genes Dev.* **14,** 2831–2838
16. Grefhorst, A., Elzinga, B. M., Voshol, P. J., Plösch, T., Kok, T., Bloks, V. W., van der Sluijs, F. H., Havekes, L. M., Romijn, J. A., Verkade, H. J., and Kuipers, F. (2002) *J. Biol. Chem.* **277,** 34182–34190
17. Chu, K., Miyazaki, M., Man, W. C., and Ntambi, J. M. (2006) *Mol. Cell Biol.* **26,** 6786–6798
18. Joseph, S. B., Laffitte, B. A., Patel, P. H., Watson, M. A., Matsukuma, K. E., Walczak, R., Collins, J. L., Osborne, T. F., and Tontonoz, P. (2002) *J. Biol. Chem.* **277,** 11019–11025
19. Talukdar, S., and Hillgartner, F. B. (2006) *J. Lipid Res.* **47,** 2451–2461
20. Chen, G., Liang, G., Ou, J., Goldstein, J. L., and Brown, M. S. (2004) *Proc. Natl. Acad. Sci. U.S.A.* **101,** 11245–11250
21. Repa, J. J., Liang, G., Ou, J., Bashmakov, Y., Lobaccaro, J. M., Shimomura, I., Shan, B., Brown, M. S., Goldstein, J. L., and Mangelsdorf, D. J. (2000) *Genes Dev.* **14,** 2819–2830
22. Cha, J. Y., and Repa, J. J. (2007) *J. Biol. Chem.* **282,** 743–751
23. Hsu, J. J., Lu, J., Huang, M. S., Geng, Y., Sage, A. P., Bradley, M. N., Tontonoz, P., Demer, L. L., and Tintut, Y. (2009) *FEBS Lett.* **583,** 1344–1348
24. Zhang, Y., and Edwards, P. A. (2008) *FEBS Lett.* **582,** 10–18
25. Lefebvre, P., Cariou, B., Lien, F., Kuipers, F., and Staels, B. (2009) *Physiol. Rev.* **89,** 147–191

26. Bishop-Bailey, D., Walsh, D. T., and Warner, T. D. (2004) *Proc. Natl. Acad. Sci. U.S.A.* **101,** 3668–3673
27. Miyazaki-Anzai, S., Levi, M., Kratzer, A., Ting, T. C., Lewis, L. B., and Miyazaki, M. (2010) *Circ. Res.*, 1807–1817
28. Chiang, J. Y. (2002) *Endocr. Rev.* **23,** 443–463
29. Watanabe, M., Houten, S. M., Wang, L., Moschetta, A., Mangelsdorf, D. J., Heyman, R. A., Moore, D. D., and Auwerx, J. (2004) *J. Clin. Invest.* **113,** 1408–1418
30. Hannah, V. C., Ou, J., Luong, A., Goldstein, J. L., and Brown, M. S. (2001) *J. Biol. Chem.* **276,** 4365–4372
31. Kim, J. B., and Spiegelman, B. M. (1996) *Genes Dev.* **10,** 1096–1107
32. Venkateswaran, A., Laffitte, B. A., Joseph, S. B., Mak, P. A., Wilpitz, D. C., Edwards, P. A., and Tontonoz, P. (2000) *Proc. Natl. Acad. Sci. U.S.A.* **97,** 12097–12102
33. Miyazaki, M., Flowers, M. T., Sampath, H., Chu, K., Otzelberger, C., Liu, X., and Ntambi, J. M. (2007) *Cell Metab.* **6,** 484–496
34. Sampath, H., Miyazaki, M., Dobrzyn, A., and Ntambi, J. M. (2007) *J. Biol. Chem.* **282,** 2483–2493
35. Giachelli, C. M., Speer, M. Y., Li, X., Rajachar, R. M., and Yang, H. (2005) *Circ. Res.* **96,** 717–722
36. Wei, Y., Wang, D., Topczewski, F., and Pagliassotti, M. J. (2006) *Am. J. Physiol. Endocrinol. Metab.* **291,** E275–281
37. Erbay, E., Babaev, V. R., Mayers, J. R., Makowski, L., Charles, K. N., Snitow, M. E., Fazio, S., Wiest, M. M., Watkins, S. M., Linton, M. F., and Hotamisligil, G. S. (2009) *Nat. Med.* **15,** 1383–1391
38. Lee, J. Y., Zhao, L., Youn, H. S., Weatherill, A. R., Tapping, R., Feng, L., Lee, W. H., Fitzgerald, K. A., and Hwang, D. H. (2004) *J. Biol. Chem.* **279,** 16971–16979
39. Lee, J. Y., Ye, J., Gao, Z., Youn, H. S., Lee, W. H., Zhao, L., Sizemore, N., and Hwang, D. H. (2003) *J. Biol. Chem.* **278,** 37041–37051
40. Lee, J. Y., Sohn, K. H., Rhee, S. H., and Hwang, D. (2001) *J. Biol. Chem.* **276,** 16683–16689
41. Lee, J. Y., Plakidas, A., Lee, W. H., Heikkinen, A., Chanmugam, P., Bray, G., and Hwang, D. H. (2003) *J. Lipid Res.* **44,** 479–486
42. Listenberger, L. L., Ory, D. S., and Schaffer, J. E. (2001) *J. Biol. Chem.* **276,** 14890–14895
43. Shimabukuro, M., Ohneda, M., Lee, Y., and Unger, R. H. (1997) *J. Clin. Invest.* **100,** 290–295
44. El-Assaad, W., Joly, E., Barbeau, A., Sladek, R., Buteau, J., Maestre, I., Pepin, E., Zhao, S., Iglesias, J., Roche, E., and Prentki, M. (2010) *Endocrinology* **151,** 3061–3073
45. Shimabukuro, M., Higa, M., Zhou, Y. T., Wang, M. Y., Newgard, C. B., and Unger, R. H. (1998) *J. Biol. Chem.* **273,** 32487–32490
46. Shimabukuro, M., Wang, M. Y., Zhou, Y. T., Newgard, C. B., and Unger, R. H. (1998) *Proc. Natl. Acad. Sci. U.S.A.* **95,** 9558–9561
47. Koshkin, V., Dai, F. F., Robson-Doucette, C. A., Chan, C. B., and Wheeler, M. B. (2008) *J. Biol. Chem.* **283,** 7936–7948
48. Listenberger, L. L., Han, X., Lewis, S. E., Cases, S., Farese, R. V., Jr., Ory, D. S., and Schaffer, J. E. (2003) *Proc. Natl. Acad. Sci. U.S.A.* **100,** 3077–3082